Catalysis Today 175 (2011) 100–105

Contents lists available at ScienceDirect

Catalysis Today

journal homepage: www.elsevier.com/locate/cattod

The role of potassium in K/Co_3O_4 for soot combustion under loose contact

Min Sun, Li Wang*, Bingnan Feng, Zhigang Zhang, Guanzhong Lu, Yun Guo*

Lab for Advanced Materials, Research Institute of Industrial Catalysis, East China University of Science & Technology, Shanghai 200237, China

ARTICLE INFO

Article history:
Received 31 October 2010
Received in revised form 10 April 2011
Accepted 23 April 2011
Available online 31 May 2011

Keywords:
Soot combustion
K/Co_3O_4
Loose contact
Catalytic activity

ABSTRACT

This work investigated the effect of potassium (K) on the catalytic activity of Co_3O_4 prepared by sol–gel method for soot combustion under loose contact. The catalysts were characterized by XRD, TPR, Raman, FT-IR, and XPS. The results showed the deposition of 4.4 wt.% K accelerated the activity of Co_3O_4 for soot combustion under loose contact, the temperature of maximum soot oxidation rate (Tm) decreased from 490 °C over Co_3O_4 to 417 °C over $K(0.1)/Co_3O_4(600)$. It was discovered that there is an exact linear relationship between Tm and the value of active Co^{3+}/Co for the first time, where Co represented the total amount Co^{3+} and Co^{2+}. Our findings strongly suggested that potassium, as a promoter, not only favors CB–catalyst contact, but also produces more active Co^{3+} with the increase of K content. Doped K entered the crystal lattice and aroused the lattice distortion. The Tm in TPO decreased linearly with the increase of microstrain. The lattice distortion and the interaction of K and Co_3O_4 promoted the formation of the surface active Co^{3+} and active O^-, and improved the activity of lattice oxygen.

1. Introduction

The purification of exhaust emissions of diesel vehicles, especially particulate materials (PM), has now been a major challenge for environmental protection [1]. The particulate emission, particularly soot, can be removed by the application of soot filter. It is very important for the regeneration of filter because the overfilled filter can damage the engine through the excessive exhaust back pressure. One of the solutions is to deposit the catalyst with good performance on the wall of filters, on which the soot can be retained and oxidized continuously. However, oxidation catalysts require a high performance at low temperatures since the temperature of diesel tailpipe falls in the range of 200–450 °C [2–5].

Many investigations have shown that some oxides, such as CeO_2, Co_3O_4 and CuO exhibit a high activity for soot catalytic combustion [6–8]. In recent years, as an excellent catalyst for low temperature CO oxidation [9], Co_3O_4 and Co_3O_4-based mixed oxide catalysts have attracted much attention due to its strong redox ability [8,10].

Excellent oxidation and mobility of the active phase are two keys for a good catalyst design. The activity and selectivity of Co_3O_4 catalyst are related to its strong redox ability of CoO_x [11]. A key obstacle to low temperature activity is the poor contact condition between soot and catalysts in the low temperature regime [2,12–14]. One of the promising candidates to burn off soot is alkaline compounds and alkali doped materials [13,15–19], especially potassium-containing materials due to their high mobility [20–26].

Several studies [12,20,27] do agree that K, as an electron donor, shows positive effects on soot combustion due to the formation of low melting point compounds or eutectics, which improve the mobility of the active species and favor the soot–catalyst contact.

Querini et al. [3,13] investigated the activity of Co or Co–K supported on MgO and proposed a redox mechanism directly related to the reducibility of cobalt. Miró et al. [27,28] studied the activity of Co–K supported on MgO, CeO_2 and La_2O_3 and found that potassium greatly promoted soot combustion involving surface carbonate species. Moggia et al. [29] reported that Co, K/La_2O_3 catalysts showed the highest catalytic activity with the highest content of surface carbonated species.

However, considering that many previous studies have systematically investigated cobalt oxide for soot combustion, the study of this reaction mechanism remains difficult to address and what we know about the combustion process on this catalyst is still limited. Although tight contact mode favors the evaluation of intrinsic kinetics [30,31], realistic soot–catalyst contact condition (loose contact) is necessary for the design of a rational catalyst in a real application.

In this paper, K/Co_3O_4 catalysts with different K contents were prepared and the catalytic performance under loose contact was evaluated. The effect of K on the structural and surface properties, redox properties and catalytic activity of Co_3O_4 was also investigated.

* Corresponding authors. Tel.: +86 21 64253703; fax: +86 21 64253824.
E-mail addresses: wangli@ecust.edu.cn (L. Wang), yunguo@ecust.edu.cn (Y. Guo).

0920-5861/$ – see front matter © 2011 Elsevier B.V. All rights reserved.
doi:10.1016/j.cattod.2011.04.044

2. Experimental

2.1. Catalyst preparation

K/Co_3O_4 catalysts were prepared by a sol–gel method. An appropriate amount of $Co(NO_3)_2{\cdot}6H_2O$, citric acid and the required amount of potassium nitrate were dissolved into de-ionized water. The amount of KNO_3 was decided by the K/Co molar ratio. The mixed aqueous solution was evaporated under stirring until the transparent gel was formed. The resulting gel was dried at 100 °C for 2 h, followed by the decomposition at 450 °C for 2 h to remove organics and the final calcinations at 600 °C for 3 h under static air. After grinding, the catalyst powder was obtained. The K/Co_3O_4 catalysts prepared was marked as K(x)/Co(600), in which x represented the molar ratio of K/Co (x = 0.02, 0.04, 0.1, 0.2 and 1.0). The real contents of K in different catalysts were measured by ICP-AES instrument (Varian 710).

2.2. Catalyst characterization

The powder X-ray diffraction (XRD) pattern analysis was performed on a Bruker D8 powder diffractometer using Cu Kα radiation (40 kV and 40 mA). The diffractograms were recorded in the 2θ range of 10–80° with a 2θ step size of 0.02° and a scanning speed of 6° min^{-1}. Rietveld refinements were carried out with the program Jade 5.0 and the average crystal size (D) and lattice microstrain of the catalysts were determined by the expressions of Scherrer and Stokes and Wilson, respectively.

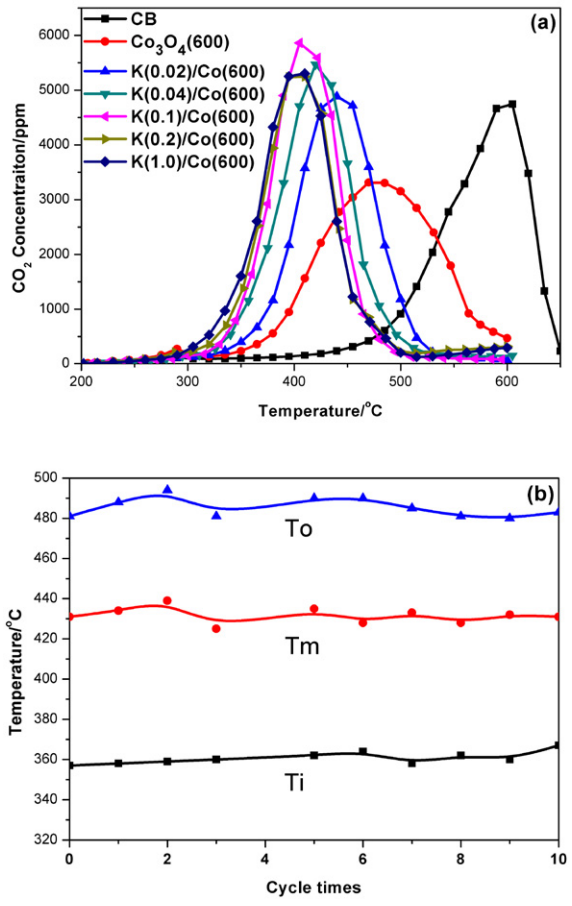

Fig. 1. (a) The direct TPO of CB and TPO profiles of CB over Co_3O_4 and K(x)/Co(600) catalysts, and (b) the TPO stabilities of the K(0.1)/Co(600) in 10 times of TPO recycles.

The XPS spectra were acquired with a Thermo ESCALAB 250 spectrometer by using Al Kα ($h\nu$ = 1486.6 eV) radiation as the excitation source. Charging of samples was corrected by setting the binding energy of adventitious carbon (C 1s) at 284.8 eV.

Hydrogen Temperature Programming Reduction (H_2-TPR) measurements were carried out using a commercial temperature-programming system. 30 mg catalyst was heated in the flow of 5 vol.% H_2/N_2 (45 ml/min) at a heating rate of 10 °C/min from 100 to 550 °C. The amount of H_2 uptake during the reduction was measured by thermal conductivity detector (TCD).

Raman spectra were recorded with thin wafer on a Renishaw spectrometer using a 514 nm Ar^+ laser as the excitation source. The laser beam intensity and the spectrum slit width were 2 mW and 3.5 cm^{-1}, respectively.

2.2.1. Catalyst evaluation

Commercially available carbon black (CB) (Printex-U Degussa: 97.23 wt.% C, 0.73 wt.% H, 1.16 wt.% O, 0.19 wt.% N, 0.45 wt.% S) was used as a model soot. The activity of catalyst for CB oxidation was evaluated in a stainless steel tube fixed-bed reactor at atmospheric pressure with a reaction gas of 8% O_2/Ar at a constant rate of 100 ml min^{-1}. The amount of sample was maintained constant at 50 mg with a CB/catalyst mass ratio of 1/9. 5.0 mg of CB was mixed with 45.0 mg of the catalyst in an agate mortar with a spatula for 2 min in order to achieve "loose" soot–catalyst contact. 200 mg of SiO_2 granules (0.3–0.5 mm) were also added to the mixture to reduce the pressure drop and to prevent thermal runaways. A K-type thermalcouple was finally inserted in the fixed-bed to detect the bed temperature. The reaction temperature was heated from 200 °C to 600 °C at a 5 °C min^{-1} rate after the pretreatment at 200 °C for 30 min under Ar flow.

The same procedure was also used to evaluate the carbon thermal reduction of catalyst using pure Ar instead of 8% O_2 in Ar.

3. Results

3.1. Carbon black catalytic oxidation on K/Co_3O_4

Fig. 1(a) shows the temperature programmed oxidation (TPO) profiles of CB over the K(x)/Co(600) catalysts under the loose contact. For the TPO of pure CB, Ti (the ignition temperature of oxidation) and Tm (maximum soot oxidation rate temperature) were 475 and 600 °C, respectively. The catalysts can remarkably accelerate the CB oxidation significantly, and the Ti and Tm over Co_3O_4 decreased to 350 and 490 °C, respectively. The catalyst activities were further enhanced after the deposition of K. The activities of K(x)/Co(600) catalysts for CB oxidation increased with the increase of K content up to 4.4 wt.% (K/Co = 0.1). To increase the K content continuously to K/Co = 1.0, the catalyst showed almost similar activities for CB oxidation. K(0.1)/Co(600) exhibited the highest activity with the Tm of 417 °C. At the same time, the K(x)/Co(600) catalysts showed good selectivity for soot oxidation, and CO was not detected during the experiments.

K(0.1)/Co(600) showed high stability for CB oxidation (Fig. 1(b)). The temperature of Ti, Tm and To (complete conversion of CB) kept nearly stable during the 10 times over recycle tests, in which the CB was re-added to catalyst bed after the complete oxidation of CB.

3.2. Catalyst characterization

XRD patterns in Fig. 2 showed that Co_3O_4 prepared had single spinel-type structure. The diffraction peaks of K(x)/Co(600) with lower K content (K/Co < 0.2) were similar with that of Co_3O_4, the characteristic peaks of K species were not observed. The phases of KNO_3 and K_2CO_3 were observed with a further increase of K

Table 1
The structure parameters of Co_3O_4 and K/Co(600) determined by XRD.

Sample	Phases	D_{311} (nm) Scherrer	Lattice parameter (Å)	Microstrain (%)	K (wt.%)[a]
Co_3O_4(600)	Spinel	34	8.060	–	–
K(0.02)/Co(600)	Spinel	35	8.066	0.0214	0.57
K(0.04)/Co(600)	Spinel	37	8.071	0.0461	1.4
K(0.1)/Co(600)	Spinel	33	8.072	0.0621	3.9
K(0.2)/Co(600)	Spinel, KNO_3	32	8.068	0.0698	7.1
K(1.0)/Co(600)	Spinel, K_2CO_3	29	8.049	0.0784	20

[a] The content of K was measured by ICP-AES.

content. It indicated that K was highly dispersed on the surface of Co_3O_4 or entered the lattice of Co_3O_4. It was reasonable to believe that some K species probably existed as KNO_3 and K_2CO_3 on the surface of Co_3O_4, although it cannot be detected over K(x)/Co(600) with lower K loading. The phase structures of K(x)/Co(600) with different K contents are listed in Table 1.

At the same time, the characteristic peak of Co_3O_4 shifted to lower 2θ degree after the deposition of K, which indicated some K inserted the lattice of Co_3O_4 and aroused the increase of lattice constant due to the larger ion radius of K. The lattice constants of samples calculated by Rietveld refinement are listed in Table 1. The deposition of K increased the lattice constant of Co_3O_4 significantly, and K(0.1)/Co(600) showed the largest lattice expansion, which implied the obvious lattice distortion and microstrain of K(0.1)/Co(600). The microstrain of K(x)/Co(600) catalysts obtained by Stokes and Wilson method are listed in Table 1. It can be seen that the microstrain of K(x)/Co(600) increased with the increase of K content.

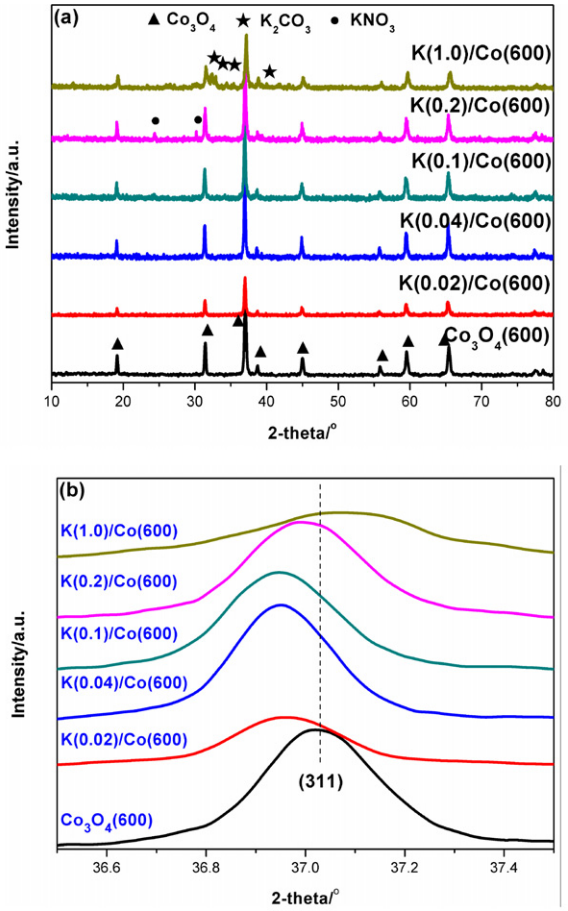

Fig. 2. XRD of Co_3O_4 and K(x)/Co(600).

H_2-TPR was used to examine the redox properties of Co_3O_4 and K(x)/Co(600) with different K loadings, and the results are shown in Fig. 3. For the TPR of Co_3O_4, a broad reduction peak was observed in the temperature range of 300–450 °C. Arnoldy and Moulijn [32] observed a single step reduction of Co_3O_4. Viswanathan and Gopalakrishnan [33] reported that the reduction of Co_3O_4 was a two-step process. After the deposition of K, the broad reduction peak split into two peaks. The first reduction peak in the range of 250–350 °C can be attributed to the reduction of Co^{3+} to Co^{2+} dispersed in the Co_3O_4 phase, while the latter one around 400 °C corresponded to the reduction of Co^{2+} ions [34,35]. At the same time, the first reduction peak shifted to the lower temperature obviously with the increase of K/Co up to 0.1. However, this reduction peak shifted to higher temperature with the further increase of K content. K(0.1)/Co(600) exhibited the lowest temperature reduction peak, corresponding to the highest activity for CB oxidation.

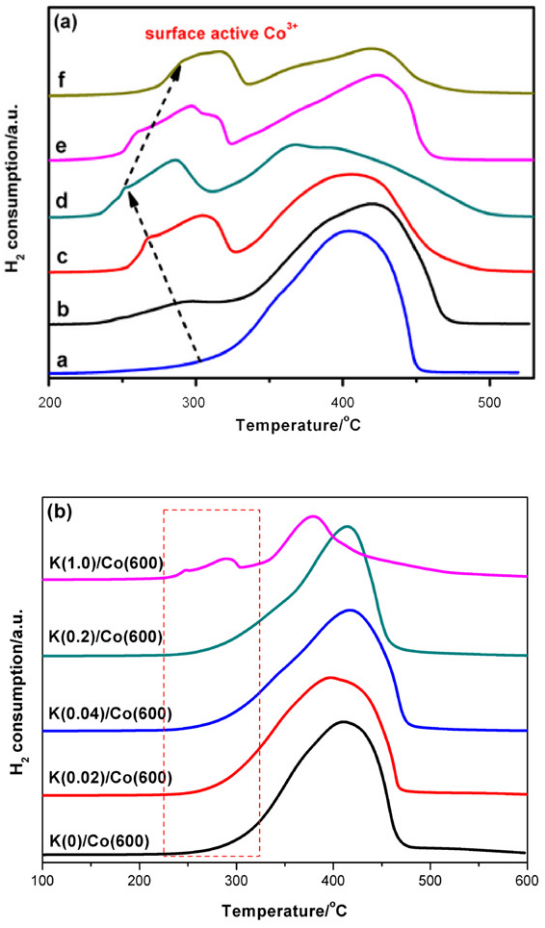

Fig. 3. (a) H_2-TPR of K(x)/Co(600): (a) 0; (b) 0.02; (c) 0.04; (d) 0.1; (e) 0.2; (f) 1.0 and (b) H_2-TPR of the mixture of CB and K(x)/Co_3O_4(600) pretreated at 400 °C under Ar flow.

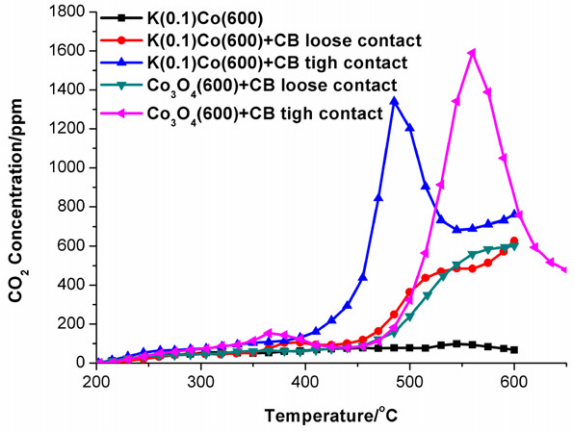

Fig. 4. Carbon thermic reduction of K(0.1)/Co(600) and Co_3O_4 under loose and tight contacts.

Moreover, in order to confirm the role of Co^{3+} and Co^{2+} in the TPO of CB over different catalysts, the TPR experiments were performed after the pretreatment of the mixed CB and catalyst in Ar at 400 °C for 0.5 h, the results are shown in Fig. 3(b). The low reduction peak ascribed to the reduction of Co^{3+} in Fig. 3(a) disappeared, which indicated the elimination of Co^{3+} in the process of pretreatment due to its reaction with CB. It was implied that the Co^{3+} played more important role than Co^{2+} in the CB catalytic oxidation.

To investigate the activity of lattice oxygen on K(x)/Co(600) catalysts, the carbon thermal reduction of catalysts in the flow of pure Ar under loose and tight contacts were performed, and the results are shown in Fig. 4. For the reaction under loose contact, K(0.1)/Co(600) showed similar activity as Co_3O_4. However, K(0.1)/Co(600) showed significantly higher activity than Co_3O_4 under the tight contact, and the Tm decreased from 560 °C on Co_3O_4 to 475 °C on K(0.1)/Co(600). Haneda et al. [36] reported that traces of added alkali metals could weaken the Co–O bond strength and promote the oxygen desorption from Co_3O_4 due to the interaction with alkali metals. Together with the TPR results, it could be drawn that the activity of lattice oxygen could be improved on K(0.1)/Co(600) due to the strong interaction between K and surface Co species (or Co_3O_4).

The Raman spectra of Co_3O_4 and K(x)/Co are shown in Fig. 5. For pure Co_3O_4, four Raman peaks at 482, 520, 620 and 692 cm^{-1} were observed clearly, which corresponds, respectively, to the E_g, F^2_{2g}, F^3_{2g} and A_{1g} modes of crystalline Co_3O_4 [37]. K(x)/Co(600) showed a similar Raman spectra with that of Co_3O_4, but the vibrations of Co_3O_4 shifted to higher frequencies with the increase of K content. Lopes et al. [38] reported that the shift of Co_3O_4 vibration was induced by the change of unit-cell parameter and particle size. The Raman results indicated the lattice constant expansion of Co_3O_4 after doping K, which coincided with the results of XRD.

Fig. 6 shows the XPS spectra of O 1s and Co 2p on different catalysts. The broad O 1s spectra on all samples indicated the existence of several kinds of surface oxygen species [39]. The species α and β at the binding energies of ca. 529.8 and 531.4 eV can be attributable to lattice O^{2-} and surface O^- species, respectively [40]. The quantitative XPS analysis is listed in Table 2.

Table 2
Surface composition of the K(x)/Co(600) after different treatment as determined by XPS.

Sample	Treatments	Co^{3+}/Co^a	K/Co^a	O^-/Co^a
K(0.04)/Co(600)	Fresh	0.39	0.19	0.57
K(0.1)/Co(600)	Fresh	0.45	0.22	0.61
K(0.1)/Co(600)+CB	430 °C, 8% O_2/Ar	0.44	0.84	1.19

[a] The total amount of Co^{3+} and Co^{2+}.

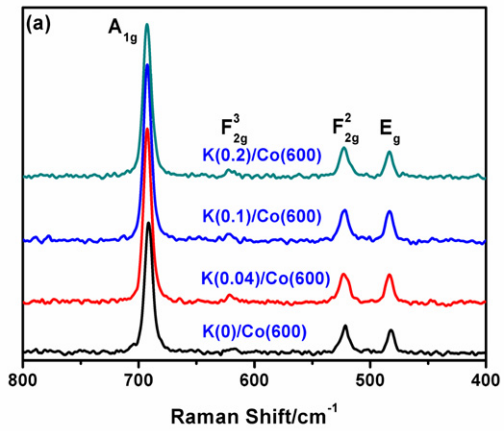

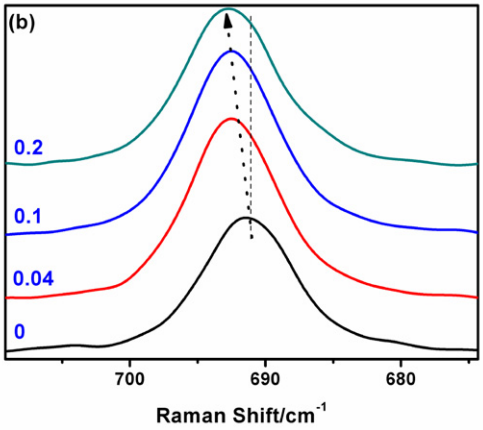

Fig. 5. Raman spectra of Co_3O_4 and K(x)/Co(600) catalysts.

The surface atomic concentrations of O^- and Co^{3+} increased with the increase of K content. After the pretreatment of mixture of K(x)/Co and CB in 8%O_2/Ar at 430 °C, surface Co^{3+} remained nearly unchanged, while the surface O^- concentration increased significantly, which demonstrated that more O^- species were produced during the reaction. In addition, the surface K/Co ratio was higher than that expected from the bulk composition, which revealed the surface richness of K. The surface enrichment of K can be promoted significantly after the pretreatment in the reaction gas corresponding to the increase of K/Co ratio due to its high mobility.

Some researchers suggested that the surface carbonate species played an important role in the soot oxidation [41]. In order to investigate the oxidation of soot by consuming the carbon to form carbonate species, the K_2CO_3/Co(600) and K(0.1)/Co(600) catalysts were analyzed by FT-IR before and after 10 reaction cycles presented in Fig. 7. The adsorption peaks at 570 and 660 cm^{-1} on all samples belong to the characteristic peaks of spinel Co_3O_4 and peaks at 3440 (not shown in Fig. 7) and 1640 cm^{-1} correspond to the surface absorbed water. For K_2CO_3/Co(600), the adsorption peak at 1390 cm^{-1} was associated with the surface carbonate potassium. The two new broad peaks at 1086 cm^{-1} and 460 cm^{-1} were detected on K_2CO_3/Co(600) after reaction, which can be signed to a carbonate-type intermediate on the surface involving the reaction [42]. The peaks at 1387 and 830 cm^{-1} on K(0.1)/Co(600) were assigned to the surface nitrate species, which were induced by the undecomposed nitrate salts in the process of catalyst preparation. The adsorption peaks of free nitrate can still be observed on K(0.1)/Co(600) after 10 reaction cycles, but its intensity decreased slightly. It indicated that the surface nitrate species participated in the soot oxidation and owned relatively high

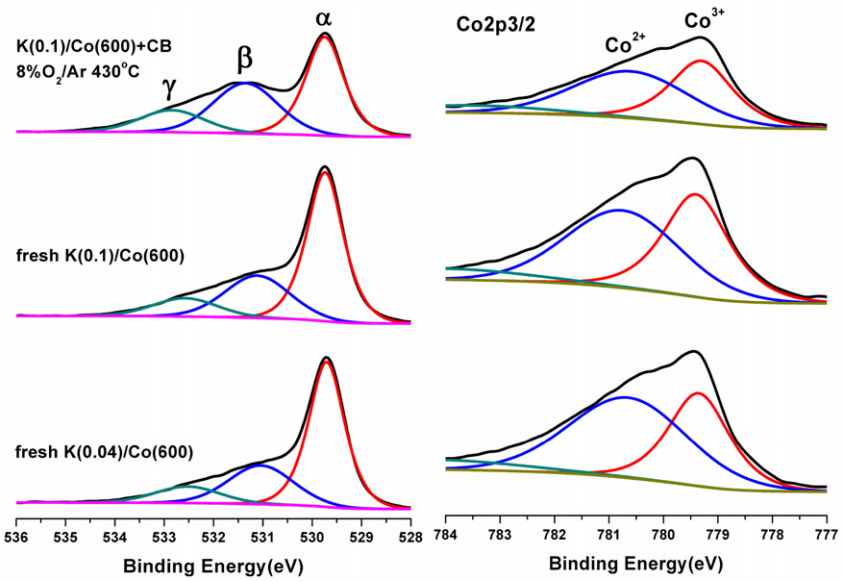

Fig. 6. XPS spectra of O 1s and Co 2p on fresh K(0.04)/Co(600), fresh K(0.1)/Co(600) and K(0.1)/Co(600) + CB pretreated at 430 °C in 8% O_2/Ar for 0.5 h.

stability. At the same time, a new adsorption peak at 1100 cm^{-1} was observed on the used K(0.1)/Co(600), which was similar to that over K_2CO_3/Co(600) and ascribed to the surface carbonate-type intermediate. It was suggested that the CB oxidation occurs by mainly forming a carbonate-type intermediate, which instantaneously decomposes in the oxidation temperature range.

4. Discussion

Co_3O_4 with outstanding redox ability is a good candidate for CB combustion. The K-doping usually promotes the catalyst activity for soot oxidation due to its high mobility, favoring the contact between catalyst and soot [27,43]. As expected, the deposition of K significantly promoted the activity of Co_3O_4 for CB oxidation, and the activity of catalyst increased with the increase of K content (Fig. 1).

XRD results showed that some doped K entered the lattice of Co_3O_4, and some existed on the surface in the form of K_2CO_3 or KNO_3. The K species in the form of salts inclined to highly disperse on the catalyst surface provides better contact condition for CB oxidation due to its high mobility. XPS results showed the surface richness of K on the K(x)/Co(600). For example, the surface K/Co ratio of K(0.04)/Co(600) and K(0.1)/Co(600) were 0.19 and 0.22, which were 4.8 and 2.2 times of that in bulk, respectively. The surface concentration of K can be further improved greatly after the reaction. These results suggested that under reaction condition, highly mobile K species can accommodate underneath or nearby the soot particles, promote the contact between catalyst and CB, and accelerate the CB oxidation.

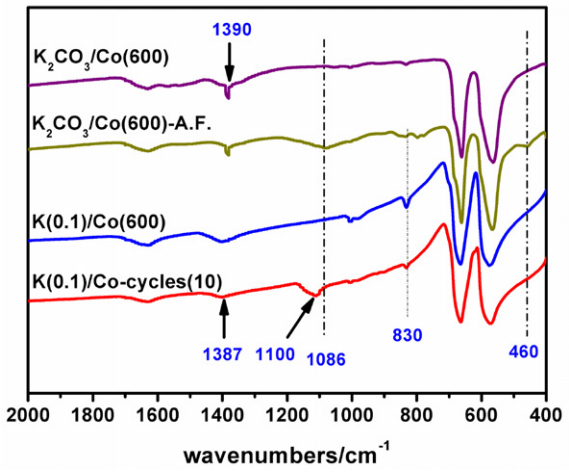

Fig. 7. FT-IR spectra of K_2CO_3/Co(600) and K(0.1)/Co(600) (A.F. = after reaction).

In the oxidation reaction, Co^{3+} was generally regarded as active site [9], and the redox ability of Co^{3+} has great effects on the catalytic activity. In H_2-TPR, a new reduction peak at the lower temperature (250–350 °C) induced by the deposition of K can be ascribed to the reduction of Co^{3+}, and the peak area increased with the increase of K content. Meanwhile, the reduction peak at low temperature decreased significantly after the pretreatment of catalyst and CB mixture at 400 °C in pure Ar. In fact, the reduction at lower temperature range was difficult to be observed on K(x)/Co(600) except on K(1.0)/Co(600). It indicated that the Co^{3+} species corresponding to the low temperature reduction can be ascribed to active Co^{3+} species and played a key role in the soot oxidation. The peak area ratio of low temperature reduction peak and the total reduction peak was used to characterize the percentage of active Co^{3+} in the total Co species.

Combining TPR and TPO, a straightforward relationship between Tm and the value of active Co^{3+}/Co was observed in Fig. 8 (blue line), where Co represented the total amount of Co^{3+} and Co^{2+}. It was implied that the activity of Co^{3+} and the amount of active Co^{3+} directly affected the catalytic activity of catalysts for CB oxidation. The increase of active Co^{3+} with the increasing of K content revealed that the deposition of K can produce more active Co^{3+}, corresponding to the increase of surface concentration of Co^{3+} in XPS.

Furthermore, the XRD and Raman results showed the deposition of K can arouse the lattice distortion of Co_3O_4 due to the insertion of K into Co_3O_4 lattice, and increase the inner microstrain with the increase of K content. It was very interesting that the Tm in TPO decreased linearly with the increase of microstrain in Fig. 8 (red line).

Liu et al. [44] investigated the total oxidation of propane on Co_3O_4, and found the amount of active O^- was an approximately linear function of the lattice microstrain due to the lattice distortion. Krishna et al. [45] reported that the activation of oxygen and

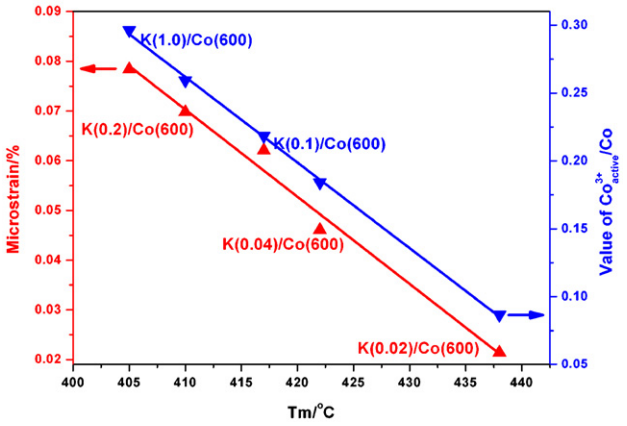

Fig. 8. The relationship between (▲) Tm and microstrain and (▼) Tm and value of $Co^{3+}{}_{active}/Co^{*}$ ($^{*}Co^{3+}{}_{active}/Co$ was determined by the H_2-TPR in Fig. 3). (For interpretation of the references to color in this figure legend, the reader is referred to the web version of the article.)

spill over of active oxygen from gas by the catalyst to soot particles are important intermediate steps in the soot oxidation. XPS results showed the surface O^- concentration increased with the increase of K content, and more O^- species can be produced in the reaction. It indicated the doped K accelerated the adsorption of oxygen and encouraged the formation of active O^-. The carbon thermic reduction experiment showed that the activity of lattice oxygen was promoted by the deposition of K.

The lattice distortion and interaction between the K and Co_3O_4 promoted the formation of more active Co^{3+} on the surface. The active Co^{3+} species on K/Co catalysts accelerated the activation of oxygen molecules and enhanced the reactivity of the active oxygen species due to the weakening of the Co–O bonds, which were suggested to be the main reasons of positive effects of K on the Co_3O_4 for soot oxidation.

The soot oxidation mechanism was reported to involve the formation of a carbonate on the catalyst, which decomposed in the range of soot oxidation temperatures [41]. In our experiments, the formation of carbonate-type species on the catalyst after the 10 reaction cycles can be detected by FT-IR, and these carbonate species kept stable in the soot oxidation. It was suggested that carbonate-type species probably was the reaction intermediate.

5. Conclusion

The K/Co_3O_4 catalysts with high catalytic performance were prepared by citrate sol–gel method and the activity of catalyst increased with the increase of K content.

The addition of K enhanced the contact condition between CB and K-containing catalysts under loose contact by the surface enrichment of K due to its high mobility.

K inserted into the lattice of Co_3O_4 can arouse the lattice distortion. With the help of the interaction between the K and Co_3O_4, the highly distorted Co_3O_4 nano-crystals weakened the Co–O bonds, and consequently improved the activity of lattice oxygen and promoted the formation of the surface active Co^{3+} sites, which were considered to accelerate the adsorption of oxygen and encourage the formation of active O^-.

Acknowledgements

This project was supported financially by the National Basic Research Program of China (2010CB732300), the National Key Technologies R & D Program of China (2007BAJ03B01), the Fundamental Research Funds for the Central Universities, and the National Natural Science Foundation of China (20601008).

References

[1] A. Carrascull, I.D. Lick, E.N. Ponzi, M.I. Ponzi, Catal. Commun. 4 (2003) 124.
[2] J.P.A. Neeft, M. Makkee, J.A. Moulijn, Appl. Catal. B: Environ. 8 (1996) 57.
[3] C.A. Querini, M.A. Ulla, F. Requejo, J. Soria, U.A. Sedrán, E.E. Miró, Appl. Catal. B: Environ. 15 (1998) 5.
[4] A.B. López, K. Krishna, M. Makkee, J.A. Moulijn, J. Catal. 230 (2005) 237.
[5] R. Cousin, S. Capelle, E. Abi-Aad, D. Courcot, A. Aboukais, Appl. Catal. B: Environ. 70 (2007) 247.
[6] P. Palmisano, N. Russo, P. Fino, et al., Appl. Catal. B: Environ. 69 (2006).
[7] Q. Liang, X.D. Wu, D. Weng, Z.X. Lu, Catal. Commun. 9 (2008) 202.
[8] P.G. Harrison, I.K. Ball, W. Daniell, P. Lukinskas, M. Céspedes, E.E. Miró, M.A. Ulla, Chem. Eng. J. 95 (2003).
[9] X. Xie, Y. Li, Z.Q.H.M. Liu, W. Shen, Nature 458 (2009) 746.
[10] M. Dhakad, T. Mitshuhashi, S. Rayalu, P. Doggali, S. Bakardjiva, J. Subrt, D. Fino, H. Haneda, N. Labhsetwar, Catal. Today 132 (2008) 188.
[11] M.M. Natile, A. Glisenti, Chem. Mater. 17 (2005) 3403.
[12] V. Serra, G. Saracco, C. Badini, V. Specchia, Appl. Catal. B: Environ. 11 (1997) 329.
[13] C.A. Querini, L.M. Cornaglia, M.A. Ulla, E.E. Miró, Appl. Catal. B: Environ. 20 (1999) 165.
[14] B.A.A.L. van Setten, J.M. Schouten, M. Makkee, J.A. Moulijn, Appl. Catal. B: Environ. 28 (2000) 253.
[15] W.F. Shangguan, Y. Teraokaa, S. Kagawaa, Appl. Catal. B: Environ. 16 (1998) 149.
[16] H. An, C. Kilroy, P.J. McGinn, Catal. Today 98 (2004) 423.
[17] B. Bialobok, J. Trawczynski, T. Rzadki, W. Mista, M. Zawadzki, Catal. Today 119 (2007) 278.
[18] D. Fino, P. Fino, G. Saracco, V. Specchia, Appl. Catal. B: Environ. 43 (2003) 243.
[19] J. Liu, Z. Zhao, C. Xu, A. Duan, T. Meng, X. Bao, Catal. Today 119 (2007) 267.
[20] S.J. Jelles, B.A.A.L. Van Setten, M. Makkee, J.A. Moulijn, Appl. Catal. B: Environ. 21 (1999) 35.
[21] P. Ciambelli, V. Palma, P. Russo, et al., Catal. Today 60 (2000) 43.
[22] G. Saracco, N. Russo, M. Ambrogio, et al., Catal. Today 60 (2000) 33.
[23] D. Fino, N. Russo, G. Saracco, V. Specchia, J. Catal. 217 (2003) 367.
[24] H. An, P.J. McGinn, Appl. Catal. B: Environ. 62 (2006) 46.
[25] P. Ciambelli, V. Palma, P. Russo, S. Vaccaro, J. Mol. Catal. A: Chem. 204 (2003) 673.
[26] J. Liu, Z. Zhao, C. Xu, A. Duan, L. Zhu, X. Wang, Appl. Catal. B: Environ. 61 (2005) 36.
[27] E.E. Miró, F. Ravelli, M.A. Ulla, L.M. Cornaglia, C.A. Querini, Catal. Today 53 (1999) 631.
[28] E.E. Miró, F. Ravelli, M.A. Ulla, L.M. Cornaglia, C.A. Querini, Stud. Surf. Sci. Catal. 130 (2000) 731.
[29] J.M. Moggia, V.G. Milt, M.A. Ulla, L.M. Cornaglia, Surf. Interface Anal. 35 (2003) 216.
[30] D. Fino, N. Russo, G. Saracco, V. Specchia, Top. Catal. 30 (2004) 251.
[31] G. Neri, G. Rizzo, S. Galvagno, A. Donato, M.G. Musolino, R. Pietropaolo, Appl. Catal. B: Environ. 42 (2003) 381.
[32] P. Arnoldy, J.A. Moulijn, J. Catal. 93 (1985) 38.
[33] B. Viswanathan, R. Gopalakrishnan, J. Catal. 99 (1986) 342.
[34] L. Spadaro, F. Arena, M.L. Granados, M. Ojeda, J.L.G. Fierro, F. Frusteri, J. Catal. 234 (2005) 451.
[35] C.W. Tang, W.Y. Yu, C.J. Lin, C.B. Wang, S.H. Chen, Catal. Lett. 116 (2007) 161.
[36] M. Haneda, Y. Kintaichi, N. Bion, H. Hamada, Appl. Catal. B: Environ. 46 (2003) 473.
[37] V.G. Hadjiev, M.N. Ilive, I.V. Vergilov, J. Phys. C: Solid State Phys. 21 (1988) 199.
[38] I. Lopes, N.E. Hassan, H. Guerba, G. Wallez, A. Davidson, Chem. Mater. 18 (2006) 5826.
[39] W. Ding, Y. Chen, X. Fu, Catal. Lett. 23 (1994) 69.
[40] M.A. Langell, F. Gevrey, M.W. Nydegger, Appl. Surf. Sci. 153 (2000) 114.
[41] M.A. Peralta, V.G. Milt, L.M. Cornaglia, C.A. Querini, J. Catal. 242 (2006) 118.
[42] S.J. Yuh, E.E. Wolf, Fuel 63 (1984) 1604.
[43] M.L. Pisarello, V. Milt, M.A. Peralta, C.A. Querini, E.E. Miró, Catal. Today 75 (2002) 465.
[44] Q. Liu, L.-C. Wang, M. Chen, Y. Cao, H.-Y. He, K.-N. Fan, J. Catal. 263 (2009) 104.
[45] K. Krishna, A. Bueno-López, M. Makkee, J.A. Moulijn, Appl. Catal. B: Environ. 75 (2007) 189.